Energy 172 (2019) 1–18

Contents lists available at ScienceDirect

Energy

journal homepage: www.elsevier.com/locate/energy

An efficient correlation for heat and mass transfer effectiveness in tumble-type clothes dryer drums

Kyle R. Gluesenkamp [a, *], Philip Boudreaux [a], Viral K. Patel [a], Dakota Goodman [b], Bo Shen [a]

[a] Building Technologies Research and Integration Center, Oak Ridge National Laboratory, One Bethel Valley Road, P.O. Box 2008, MS-6070, Oak Ridge, TN, 37831-6070, USA
[b] J.B. Speed School of Engineering, University of Louisville, 132 Eastern Pkwy, Louisville, KY, 40292, USA

ARTICLE INFO

Article history:
Received 19 September 2018
Received in revised form
20 December 2018
Accepted 28 January 2019
Available online 30 January 2019

Keywords:
Clothes dryer
Heat and mass transfer
Lewis
Buckingham pi theorem
Dimensional analysis
Effectiveness

ABSTRACT

A heat and mass transfer effectiveness definition relevant to clothes dryers is developed in this work. A correlation is presented for determining the effectiveness of heat and mass transfer in a horizontal-axis, tumble-type clothes dryer drum with axial airflow. The correlation is a function of four measurable quantities: air mass flow rate, cloth mass, air mass in the drum, and the fall time experienced by a cloth falling the full height (i.e. diameter) of the drum. The Buckingham Pi Theorem is applied to the problem in order to derive dimensionless terms upon which the effectiveness depends. Empirical data from several dryers are used to derive an empirical correlation as a function of the dimensionless variables. Three cloth types were investigated, and a separate empirical correlation is proposed for each. Together, the drum effectiveness concept and the correlation presented provide a new, more accurate, computationally efficient, and readily implemented framework for modeling and simulating clothes dryers. It is relevant to conventional gas and electric clothes drying appliances, vapor compression heat pump dryers, and thermoelectric heat pump clothes dryers. With appropriate empirical inputs, the framework is extensible to any thermal-evaporative cloth drying systems, including radial-flow horizontal axis tumble drying drums.

1. Introduction

71% of homes in the US have electric clothes dryers, which is approximately 81 million homes. Collectively, US residential clothes dryers used roughly 60 TWh/year, about 4% of the total US residential energy use in 2017 [1]. The National Resource Defense Council states the US spends 9 billion dollars each year on operating clothes dryers [2]. They also include, "A typical household pays over $100 in annual utility bills to operate an electric dryer … Homes with electric dryers pay at least $1500 over the dryer's lifetime for the electricity to power the machine" [2]. The two main types of residential clothes dryers used in the US are electric resistance (ER) and natural gas (G) dryers (75% are electric and 25% use natural gas [3]). While high-efficiency vapor-compression heat pump (VCHP) clothes dryers are available, their market penetration in the US is very low. As a result of the high annual cost and energy consumption of clothes dryers, much recent research has been dedicated to improving their energy efficiency.

Drying phenomena and their associated heat and mass transfer processes have been studied for decades [4–8]. In the analytical work of Sherwood, who studied the air drying of solids [6], two main cases were proposed to describe the drying process in solid materials which were (a.) the evaporation of water from the surface of the solid and (b.) the evaporation of water within the internal solid structure. The focus of [6] was the case where the interior resistance to liquid diffusion through the solid is large compared to the surface resistance to vapor removal. Newton's law of diffusion in an infinite sheet was solved to characterize the moisture gradients during drying of a slab of material and a simplified equation was derived to calculate the theoretical liquid distribution at any time in material where internal liquid diffusion controls the drying. The results of the theoretical drying equation fit reasonably well with experimental data for drying of wood and clay for constant drying conditions.

In later work, Sherwood [7] described the constant- and falling-rate periods of drying in solids. A "critical liquid content" point was defined, where the drying-rate began to decrease and transition to falling-rate drying. For the constant-rate drying period, the effects

* Corresponding author.
E-mail address: gluesenkampk@ornl.gov (K.R. Gluesenkamp).

https://doi.org/10.1016/j.energy.2019.01.146
0360-5442/

of adjoining dry surfaces, radiation from surroundings and air velocity on drying rate were studied. In particular, the study of adjoining dry surfaces yielded interesting results; it showed that the rate of drying of a wet solid was not decreased in proportion to the amount of surface covered by an impervious layer. The analysis showed that decreasing the wetted face area of a surface by 50% only resulted in a 20% decrease in the drying rate. For the falling-rate drying period, two distinct parts were described. In the first part, the drying rate decreased linearly because of a reduction in the wetted surface. In the second and final part, internal liquid diffusion controlled the drying process (described above), and the drying rate decreased non-linearly. Although these defined the falling-rate period well, an approximate analysis was done for use in practical drying problems. A simple equation was devised to describe the falling-rate drying period, by assuming that the rate of drying was entirely a linear function of the water content of the material. Although this was a rough approximation, the comparison to experimental data showed good agreement.

A relatively early study that used the above analysis for clothes dryer modeling was conducted by Lambert et al. [9], who created a model of an electric-resistance tumble-dryer and characterized heat and mass transfer between its various elements. The model accounted for partial recirculation of exhaust air and included a mathematical approximation of the moisture sorption isotherms for cotton, ultimately used to determine the mass transfer rate between fabric and air. Three phases of the drying process were described: initial transient, constant-rate drying and falling rate drying. Three time scales were defined for the process: the residence time of the drying air in the apparatus, characteristic time-scale for heating the fabric and the overall drying time. The model was adjusted by modifying the heat and mass transfer coefficients and sorption isotherms. The characteristic features of the drying process as predicted by the model agreed with experimental data.

Similar modeling and experimental research on fabric drying in a small domestic tumble dryer was performed by Deans [10]. In addition to characterizing the energy and mass transfer routes within the dryer, the effect of localized accumulation of lint in a trap, influence of the fabric type, sensitivity to operating conditions and energy recovery from the recirculating exhaust stream were all studied for their effect on dryer performance. A comparison between experimental results and model predictions for drying time and energy consumption showed an error of less than 8%. The performance tests showed that the distribution of clothes in the drum depended on the fabric type, packing density and moisture content, and was closely coupled to the heat and mass transfer rates. Variation of the fabric type in the model showed that the specific energy consumed in drying the load and final fabric temperature were both affected by fabric porosity.

A slightly different approach to those in Refs. [9,10] was taken by Yi et al. [11], who developed a physics-based model for thin clothes. Rather than using mathematical approximations of the sorption isotherms (based on regression of experimental data), the water activity coefficient was expressed as a function of cloth type, mass transfer rate, water latent heat and cloth temperature using statistical mechanics. With good agreement between the new model predictions and experimental data from the literature, Yi et al. could accurately predict the fabric moisture content and temperature as function of time, compared to experimental results from their clothes dryer test setup.

Bassily and Colver conducted a detailed performance analysis of an electric resistance dryer [12]. The heater power, fan speed, drum speed, weight and initial moisture content of the clothes were varied over 32 experimental runs. The data from the comprehensive experimental study were used to develop a correlation for the area-mass transfer coefficient inside the dryer drum [13]. The Sherwood number was defined and correlated to the weight of clothes, drum speed, Reynolds number, Schmidt number, and Gukhman number using the experimental data. The correlation equation showed that the mass transfer area is a function of the weight of the clothes and drum rotation speed, while the mass transfer coefficient is a function of the air flow rate, the drum outlet RH and temperature and fabric type. An increase in the inlet air temperature increased the mass transfer coefficient. To obtain a measure of efficiency of the mass transfer process, an “ideal” mass transfer process was experimentally studied, wherein a stretched, wet piece of fabric was held perpendicularly to an incoming air stream. The comparison between the actual and ideal process showed that the mass transfer efficiency averaged 26.4% during the 32 experimental runs.

Similarly, Yadav and Moon [14] performed a modeling and experimental study on a compact tumble-dryer. The model accounted for all the major components of the dryer and three time-scales were proposed, similar to those in Ref. [9]. The mass transfer coefficient was characterized as a function of the heat transfer coefficient and Lewis number. Various model input parameters were used to compute the temperature and moisture levels for the air at the drum exit at each time level, along with the total drying time. Experiments performed on the instrumented clothes dryer were based on three major national and global test standards, which accounted for variation in load size/type, initial/final moisture content, and ranges for ambient conditions. A common basis for comparison of dryer performance among the different standards was the specific moisture extraction rate (SMER), which was the electric energy consumed to remove 1 kg of moisture from the load. The overall comparison between experimental and numerical results for SMER were in fair agreement for the different standards. The work was also used to develop an empirical correlation to evaluate SMER for various standards and any other combination of input parameters.

Since the SMER is known to be a relatively consistent measure of dryer performance, other researchers such as Strawreberg and Nilsson [15], have focused on finding the clothes dryer settings and operating conditions which maximize it. In addition to developing a simplified physical model (like others in the literature), they used the Design of Experiments (DOE) methodology to create a statistical model of a condensing tumble dryer. The statistical model results indicated that the highest SMER was achieved for a high heater power, high internal air flow and low external air flow. The leakage ratio was most affected by the external air flow and there was a correlation between the moisture content of the air in the drum and the leakage ratio at different external air flows.

As shown above, many studies in the literature have accounted for the physics of heat and mass transfer for all kinds of drying. Additional thermodynamic analysis has been conducted to characterize the overall drying process efficiency, such as detailed system exergy analysis and optimization studies for industrial and agricultural drying [16–19]. However, few studies in the literature have focused on the development of an efficient correlation for the heat and mass transfer process occurring in the drum of tumble-type clothes dryers. For clothes dryers, a drum effectiveness model was first introduced by Shen et al. [20], who developed a physics-based, quasi-steady-state heat pump clothes dryer system model with detailed heat exchanger and compressor models. In a novel approach, a heat and mass transfer effectiveness model was applied to simulate the drying process of the clothes load in the drum. The system model was able to simulate the inherently transient drying process, to size components, and to reveal trends in key variables (e.g. compressor discharge temperature, power consumption, required drying time, etc). The system model was

calibrated using experimental data on a prototype heat pump clothes dryer. The model predictions were compared with experimental data measured on a prototype heat pump clothes dryer. In the present work, the heat and mass transfer effectiveness model is used along with empirical data from several different clothes dryers to develop an accurate and versatile correlation that can easily be applied to the modeling and simulation of clothes dryer performance. The empirical data was obtained from a selection of ER dryers (most commonly used dryers in the US, as noted above), along with an additional natural gas (G) dryer and a recently-developed prototype thermoelectric heat pump (TE) dryer [21] which were included to help validate the methodology used in the study.

2. Modeling approach

2.1. Definition and calculation of effectiveness

Here we derive an expression for drum heat and mass transfer effectiveness. The method used here closely follows that used by Braun et al. [22], who developed an effectiveness-based approach to model cooling towers and cooling coils and assumed that the Lewis number (Le, the ratio of mass and thermal diffusivities) had a value of 1. Both the clothes dryer drum and wet cooling tower involve an air stream which is humidified as it passes through wet media. Many cooling towers use a packing material to increase the contact surface between the air and water streams. The cooling tower packing material exposes liquid moisture to the air stream, similar to the cloth in a dryer drum. As such, the cooling tower and dryer drum have a similar heat and mass transfer process on a wet surface. Considering this, we have extended Braun's modeling approach to the dryer drum with air passing through a wet cloth load. As will be shown, the same definition of effectiveness is derived, despite the different functions of a cooling tower system (cooling water) and the dryer drum (drying cloth).

Consider the drum heat and mass transfer process and its associated differential control volume shown in Fig. 1. T_{in} and ω_{in} are the temperature and humidity ratio, respectively, of the air entering the drum. T_{out} and ω_{out} are the temperature and humidity ratio, respectively, of the air exiting the drum. T_{surf} and ω_{surf} are the temperature and humidity ratio of the cloth surface and are assumed to be uniform for all the cloth in the drum. For the differential volume, with a wet surface of differential area dA, Eq. (1) describes the sensible air energy change, where $\dot{m}_a$ is the air mass flow rate, c_p is the air specific heat, T is the air temperature, dT is the temperature change along the differential surface and h_{co} is the convective heat transfer coefficient. Similarly, Eq. (2) describes the latent air energy change, where $d\omega$ is the air specific humidity change, h_m is the mass transfer coefficient, and h_{fg} is the water latent heat of evaporation.

$$\dot{m}_a c_p dT = h_{co} dA\left(T_{surf} - T\right) \tag{1}$$

$$\dot{m}_a h_{fg} d\omega = h_m dA\left(\omega_{surf} - \omega\right) h_{fg} \tag{2}$$

Note that, as written, dT and Eq. (1) are negative (the air loses temperature and sensible heat) while $d\omega$ and Eq. (2) are positive (the air gains moisture and latent energy). For each of these ordinary differential equations (ODEs), integration across the whole surface can be applied under the assumption that the surface temperature is spatially uniform. This yields Eq. (3) for heat transfer and Eq. (4) for mass transfer:

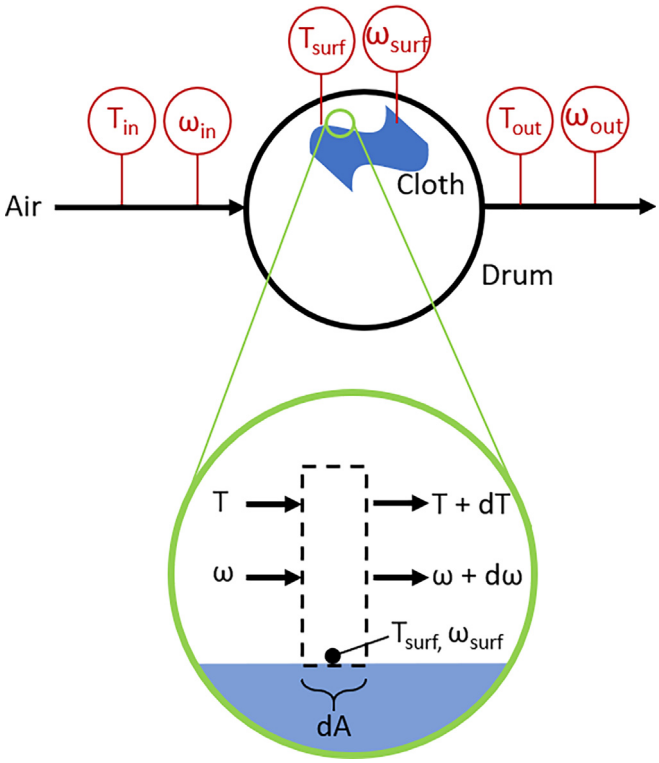

Fig. 1. Macro-level (top) and differential view (bottom) of the heat and mass transfer process in a dryer drum.

$$T_{out} = T_{surf} - \left(T_{surf} - T_{in}\right) e^{-NTU} \tag{3}$$

$$\omega_{out} = \omega_{surf} - \left(\omega_{surf} - \omega_{in}\right) e^{-NTU} \tag{4}$$

where NTU is the number of transfer units as defined in Eq. (5),

$$NTU = \frac{h_{co} A_t}{\dot{m}_a c_p} \tag{5}$$

and all other quantities are as previously defined. Based on this analysis, we see that the driving potential for heat transfer is the difference between the entering air temperature and the surface temperature at the cloth surface; the driving potential for mass transfer is the specific humidity difference between the entering air and the saturated specific humidity at the wet cloth surface temperature.

Furthermore, as shown in Eq. (6), we can describe the heat transfer effectiveness, ε_H, as the ratio of the realized heat transfer rate, Q, to the maximum possible heat transfer rate, Q_{max}. The farthest right-hand side of Eq. (6) is the form used henceforth in this work.

$$\varepsilon_H = \frac{Q}{Q_{max}} = \frac{\dot{m}_a c_p (T_{out} - T_{in})}{\dot{m}_a c_p \left(T_{surf} - T_{in}\right)} = \frac{T_{out} - T_{in}}{T_{surf} - T_{in}} \tag{6}$$

Similarly, the mass transfer effectiveness, ε_M, is defined as the ratio of the realized mass transfer rate, J, to the maximum possible mass transfer rate, J_{max}, as shown in Eq. (7), with the farthest right-hand side showing the form used henceforth in this work.

$$\varepsilon_M = \frac{J}{J_{max}} = \frac{\dot{m}_a(\omega_{out} - \omega_{in})}{\dot{m}_a\left(\omega_{surf} - \omega_{in}\right)} = \frac{\omega_{out} - \omega_{in}}{\omega_{surf} - \omega_{in}} \quad (7)$$

In this work, the drum is treated as an adiabatic enclosure, the cloth is treated as a lumped mass, and it is assumed the air stream exchanges heat and moisture with a layer of air at the cloth surface. This air at the cloth surface is treated as being saturated with moisture at the cloth surface temperature. Furthermore, the cloth temperature is treated as quasi-steady state, since the air changes state in a matter of seconds as it passes through the drum, whereas the cloth changes temperature much more slowly (over tens of minutes). From these premises, it follows that the air humidification process is isenthalpic, i.e. the air is exchanging sensible energy for latent energy in equal measure.

An additional justification for treating the cloth temperature as quasi-steady state is the relatively minor impact of its thermal mass in comparison to the total evaporation energy. An analysis of the total thermal mass of the dryer components (from air inlet to exhaust, including wet load) found that approximately 10% of electrical energy consumed by the dryer is consumed by sensible heating of dryer components and the load itself. Although non-trivial, this sensible heating is not a main effect, and is beyond the scope of this paper. Furthermore, the impact of sensible heating will disproportionately affect the initial transient and final falling rate drying phases (with greater than 10% effect during these phases). Thus, the impact of sensible heating will be substantially less during the middle constant-rate drying phase.

Using Eq. (6) and Eq. (7), heat and mass transfer effectiveness (ε_H and ε_M) can be calculated by measuring temperature (T) and humidity ratio (ω) at the drum inlet (T_{in}, ω_{in}), on the clothing surface inside the drum (T_{surf}, ω_{surf}), and at the drum exhaust (T_{out}, ω_{out}) over the duration of the dryer cycle. However, due to the difficulties of accurately measuring clothing surface temperature and humidity ratio, T_{surf} and ω_{surf} must be calculated. Equations (6) and (7) include 8 variables (ε_H, ε_M, T_{in}, T_{out}, ω_{in}, ω_{out}, T_{surf} and ω_{surf}), thus a solution of the equation set requires eight equations. Equations (6) and (7) provide two, and the next 4 are provided by measurements, as shown in Eqs. (8)–(11).

$$T_{in} = (\text{measured value}) \quad (8)$$

$$T_{out} = (\text{measured value}) \quad (9)$$

$$\omega_{in} = (\text{measured value}) \quad (10)$$

$$\omega_{out} = (\text{measured value}) \quad (11)$$

To obtain two additional equations and solve the equation set, the following two assumptions were used.

$$\varepsilon_H = \varepsilon_M \quad (12)$$

First, heat and mass transfer effectiveness are assumed to be equal, as shown in Eq. (12).

Next, the clothing surface was assumed to be saturated, as shown in Eq. (13).

$$\omega_{surf} = \omega_{surf,sat} \quad (13)$$

Equation (13) introduces a new variable, $\omega_{surf,sat}$, bringing the total number of variables to 9, and therefore requiring a ninth equation. Eq. (14) provides this final equation by describing $\omega_{surf,sat}$ as a function of saturated vapor pressure, $p_{w,sat}$, at T_{surf} and measured atmospheric pressure, p_{atm}.

$$\omega_{surf,sat} = \frac{0.62198 \cdot p_{w,sat}\big|_{T_{surf}}}{\left(p_{atm} - p_{w,sat}\big|_{T_{surf}}\right)} \quad (14)$$

Finally, effectiveness and the bulk wet surface temperature can be calculated by solving the set of 9 simultaneous equations described in Eqs. (6-14).

Engineering Equation Solver (EES) [23] software was utilized to solve this equation set at each point of time during the dryer cycle. To aid in solution convergence, upper and lower bounds for some variables were given to guide the simultaneous equation solver's computation of T_{surf} and ω_{surf}. Specifically, T_{surf} was bounded between 5 and 50 °C, and ε_H and ε_M were bounded between −0.2 and + 1.0. These were not "active constraints," i.e. no solutions shown in this work were limited by those bounds. The bounds assisted the solver to converge more quickly by avoiding non-physical mathematical solutions.

2.2. Measurement locations

Equations (6-14) utilize drum inlet and outlet conditions, and thus the most direct effectiveness calculation would use the psychrometric state immediately before and after the drum. Referring to Fig. 2, these are points ④ and ⑤. However, these measurement points are intrusive and uncommonly measured. To maximize the impact and applicability of this work, it is desirable to make use of the most widespread measurements. Psychrometric measurements of the air surrounding the cabinet and the air leaving the exhaust duct are in widespread common practice during clothes dryer evaluation (state points ① and ⑧), and can be accessed without any dryer modifications, and thus these have been used in this work. By choosing these measurement points, the effectiveness calculation methodology provided in this work can be applied to a large quantity of existing laboratory and field measurement data, for both future data and retroactively to past data.

2.3. Uncertainty analysis

The choice of indirect measurement points (ambient ① and exhaust ⑧, instead of drum inlet ④ and outlet ⑤), complicates uncertainty quantification. The effectiveness uncertainty depends on the uncertainty of the sensors used, as well as depending on unmeasured variables that influence the measurements (specifically, air leakage). In this work, this is addressed in two steps.

First, a traditional uncertainty analysis using a numerical scheme is used to quantify the uncertainty in effectiveness due to measurement uncertainties.

Second, the error introduced by unmeasured leakages is computed in a parametric study that compares the "true" effectiveness (if effectiveness were calculated based on ④ and ⑤) to the "measured" effectiveness (using the experimental measurement points chosen in this work ① and ⑧, without knowledge of leakage quantities).

In this analysis, the psychrometric impact of the blower was neglected (parameters at state point ⑦ and ⑧ are taken as equal) for the following reasons:

- Generally, dryer motors dissipate motor waste heat into the cabinet, where it is introduced to the drum and would not affect effectiveness calculation
- The air temperature rise due to actual flow work done by the blower is very small compared to typical heater power

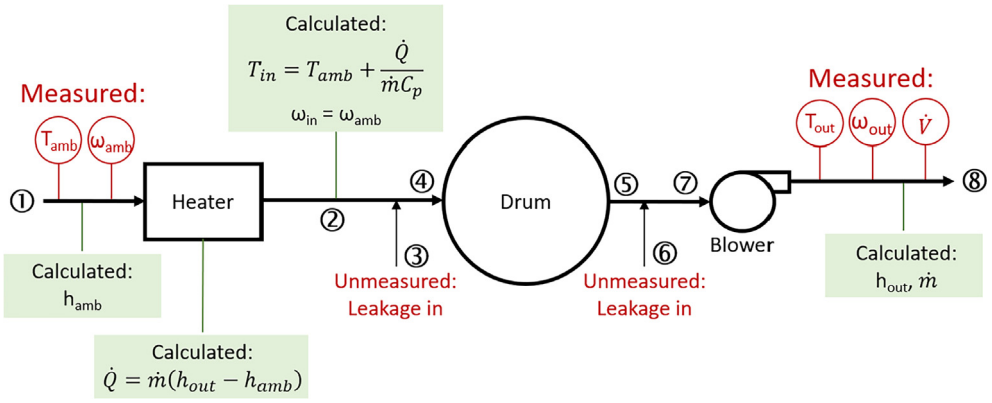

Fig. 2. Drum inlet and outlet state points.

- The pressure rise in the blower is 250–500 Pa, not a significant impact on the relevant psychrometric properties (e.g. up to a 0.2% impact on RH at a given T and ω).

2.4. Effect of measurement uncertainty

Due to the reliance on numerical psychrometric property lookups and the use of a simultaneous equation solver to calculate effectiveness, a numerical approach for uncertainty propagation was used. The inputs and results for uncertainty are shown in Table 1 for one representative case. The absolute uncertainty in non-dimensional effectiveness was 0.013. The dominant contribution to this uncertainty came from the inherent measurement uncertainty of the exhaust relative humidity transducer, which contributed 93.9% of the uncertainty, as shown in Table 1.

The full psychrometric state points for this case are shown in Table 2.

2.4.1. Effect of unmeasured leakage

An important unmeasured variable is the leakage entering the airflow, as indicated by states ③ and ⑥ in Fig. 2. The following analysis was conducted to assess the impact of leakage through these state points on the calculated effectiveness. Leakage has been shown experimentally to range from 11 to 31% in off-the-shelf dryers [24].

Starting from the definitions in Eqs. (6) and (7), two types of effectiveness were calculated: the "true" effectiveness used inlet and outlet conditions immediately adjacent to the drum (④ and ⑤). This is shown in Eqs. (15-16). Next, an "as measured" case was defined, shown in Eqs. (17-18), that utilizes the ambient and exhaust measurements as defined and used throughout this work (① and ⑧). Equations (15-18) utilize state point definitions provided in Fig. 2.

Note that T_{surf} will have one value in Eqs. (15-16), and a slightly different value in Eqs. (17-18). Similarly, ω_{surf} will have one value in Eqs. (15-16), and a slightly different value in Eqs. (17-18). The difference between Eq. (15) and Eq. (17) arises from leakages (shown in Fig. 2), which result in a slight temperature and humidity difference between ⑧ and ⑤, and a slight temperature and humidity difference between ① and ④. The same applies to the difference between Eq. (16) and Eq. (18).

$$\varepsilon_{H,true} = \frac{T_5 - T_4}{T_{surf} - T_4} \tag{15}$$

$$\varepsilon_{M,true} = \frac{\omega_5 - \omega_4}{\omega_{surf} - \omega_4} \tag{16}$$

$$\varepsilon_{H,measured} = \frac{T_8 - T_1}{T_{surf} - T_1} \tag{17}$$

$$\varepsilon_{M,measured} = \frac{\omega_8 - \omega_1}{\omega_{surf} - \omega_1} \tag{18}$$

Fig. 3 shows the "true" versus the "measured" value of effectiveness for 10,000 simulated cases. This number of cases was selected to adequately cover the operational domain with a reasonable amount of computational effort. These cases represent a 10-step (equally-spaced) full factorial in four parameters: varying drum leakage rate at ③ (1–20%), drum leakage rate ⑥ (1–20%), heat input (2–5 kW at 110 CFM), and drum outlet relative humidity

Table 1
Uncertainty results based on measurement uncertainties.

Variable	Measurement uncertainty	Value	Units	% contribution to uncertainty in effectiveness	Instrument Manufacturer and Model
Volumetric air flow rate, V [1]	5%	0.05192 ± 0.0025	m^3s^{-1}	4.9%	Air Monitor Corp. Veltron DPT2500 Transmitter with 4″ LO-flo Pitot Traverse Station
Pressure, P [1]	0.1 kPa	101.325 ± 0.1	kPa	0.0%	Setra Model 264 Very Low Differential Pressure Transducer
Heater power, Q	2%	2.50 ± 0.05	kW	0.8%	Ohio Semitronics, Inc. AC Watt Transducer
Relative humidity, RH [1]	2%RH	0.50 ± 0.02	%RH	0.1%	Vaisala HMT
Air temperature, T [1]	0.5 K	25.0 ± 0.5	°C	0.1%	Type T thermocouple
Relative humidity, RH [7]	3%RH	0.828 ± 0.030	%RH	93.9%	Vaisala HMT337 with HUMICAP 180VC heated probe
Air temperature, T [7]	0.5 K	29.3 ± 0.5	°C	0.2%	Omega SLE Type T thermocouple
Effectiveness, ε	N/A	**0.932 ± 0.013**	–	N/A	N/A

Table 2
Psychrometric state points in case evaluated for uncertainty.

		$\dot{m}_{da}$[kg$_{da}^{1}$s^{-1}]	T [°C]	RH [P$_{w}^{1}$P$_{sat}^{-1}$]	ω [g$_{w}^{1}$g$_{da}^{-1}$]	h [kJ^{1}kg$_{da}^{-1}$]	ρ [kg^{1}m^{-3}]
State point	1	0.06110	25.0	0.500	0.00988	50.27	1.177
	2	0.06110	64.9	0.063	0.00988	91.19	1.038
	3	0.00611	25.0	0.500	0.00988	50.27	1.177
	4	0.06721	61.3	0.075	0.00988	87.47	1.049
	5	0.06721	29.7	0.850	0.02255	87.47	1.150
	6	0.00672	25.0	0.500	0.00988	50.27	1.177
	7	0.07393	29.3	0.828	0.02140	84.09	1.153

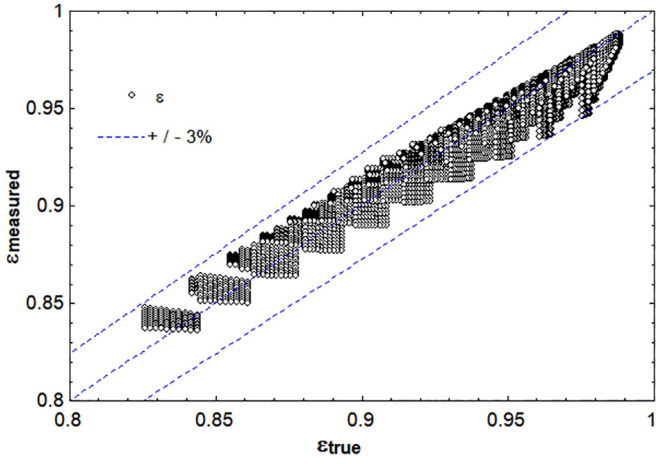

Fig. 3. The impact of unmeasured leakage on the effectiveness calculation has a maximum error of 3% for 10,000 simulated cases.

(70–95%).

In summary, the analysis based on sensor uncertainty showed a 1.3% uncertainty in effectiveness, while the analysis based on unmeasured leakage showed an average error of 0.8%, with a maximum error no greater than 3%. Thus the choice of ambient and exhaust temperatures ① and ⑧ and the instrumentation used are sufficient to capture an accurate experimental effectiveness.

3. Empirical inputs

3.1. Measured data with DOE test cloth

Data from 22 trials on 7 dryer units were used to develop the effectiveness model for standard DOE test cloth [25]. Each trial involved drying a wet cloth load from an initial moisture content (either 57% or 70% moisture) to within a few percent of bone dry. These 22 trials varied by dryer unit, load size, and air flow rate. The dryers used included electric resistance (ER), gas (G) and thermoelectric heat pump (TE) models as shown in Table 3. For the TE 1 and ER 5 units, multiple trials were conducted with varying load size and air flow rate as shown in Table 4 and Table 5.

For each trial the temperature and moisture content of the air exiting the drum was measured as well as the volumetric flow rate of the air through the drum. For trials with the TE 1 unit, temperature and moisture content of the air entering the drum were measured. For the other trials the temperature and moisture content of the air as it entered the heating element were calculated using Eqs. (19-21). This assumes that the change in energy from the ambient air entering the cabinet to the air exiting the drum (Q_{air}) can all be attributed to the energy the heater adds to the air stream (see Fig. 4), neglecting the transient heating (as described in Section 2.1). In the equations, T_{amb} and ω_{amb} are the time-dependent temperature and humidity ratio, respectively, of the ambient air entering the dryer cabinet, $\dot{m}$ is the mass flow rate of the air, h_{fg} is the latent heat of vaporization of water at temperature T_{out}, and C_p is the specific heat of moist air at the average temperature and humidity ratio of state points *in* and *out*.

$$\omega_{in} = \omega_{amb} \tag{19}$$

$$Q_{air} = \dot{m}h_{fg}(\omega_{out} - \omega_{in}) + \dot{m}C_p(T_{out} - T_{amb}) \tag{20}$$

$$T_{in} = \frac{Q_{air}}{\dot{m}C_p} + T_{amb} \tag{21}$$

Each dryer was placed on a load cell for the calculation of the remaining moisture content of the cloth throughout the drying process. Eq. (22) defines the remaining moisture content (RMC) where m_c is the mass of bone-dry cloth and m_w is the mass of water in the cloth (which changes through the drying process).

$$RMC = \left(\frac{m_w}{m_c}\right) \tag{22}$$

3.2. Trends in measured data with DOE cloth

Comparing data from different trials with the same cloth type (DOE cloth) reveals trends in effectiveness with respect to drum airflow, drum size and cloth load size. The effectiveness also changes as a function of time through the dryer cycle and can also be expressed as a function of the remaining moisture content (RMC) in the load. Fig. 5 shows the effectiveness as a function of RMC for all 22 trials. Most of these trails started with 57.5% moisture content and terminated around 2% moisture content, as can be seen by inspection of the x-axis in Fig. 5 [25]. Notice that the effectiveness decreases as the RMC decreases through the cycle. The drying process has been defined as having a constant rate drying phase and a falling rate drying phase [7]. These qualitative descriptions can be seen in the data in Fig. 5.

Two dryer characteristics which were expected to affect the effectiveness are the volumetric air flow rate and the drum volume. These parameters can be combined to define a residence time, τ, of the air in the dryer drum, shown in Eq. (23) where V is the drum volume and $\dot{V}_{da}$ is the volumetric flow rate through the drum (dry air basis). Fig. 6 shows how effectiveness changes for all trials that used a load with m_c of 3.83 kg (8.45 lb). In general, Fig. 6 shows trends of higher effectiveness for longer residence times and higher inlet temperatures.

$$\tau = \frac{V}{\dot{V}_{da}} \tag{23}$$

Another parameter that affects the heat and mass transfer effectiveness is the load size, in particular the bone-dry weight

Table 3
Dryers and loads used.

Dryer unit type and name		ER 1	ER 2	ER 3	ER 4	GA 1	TE 1	ER 5
Commercially available?		Yes	Yes	Yes	Yes	Yes	No	Yes
Number of trials used in this work	[–]	1	1	1	1	1	9	8
Drum volume	[L]	227	113	113	215	170	187	195
	[ft^3]	8.0	4.0	4.0	7.6	6.0	6.6	6.9
Drum depth	[m]	0.749	0.603	0.521	0.762	0.572	0.533	0.572
	[in]	29.5	23.75	20.5	30	22.5	21	22.5
Load size(s)	[kg]	3.83	1.36	1.36	3.83	3.83	3.83	5.90
							2.49	2.49
							2.27	1.36
							1.36	
	[lb]	8.45	3	3	8.45	8.45	8.45	13
							5.5	5.5
							5	3
							3	
Cloth type		DOE	DOE	DOE	DOE	DOE	DOE	DOE
Volumetric air flow rate	[L-s^{-1}]	69.4	35.4	44.8	54.3	59.0	Various See Table 4	Various See Table 5
	[CFM]	147	75	95	115	125		

Table 4
TE 1 model trials that vary in load size and air flow rate.

	Load size (bone dry weight)		Drum air flow	
	[kg]	[lb]	[L-s^{-1}]	[CFM]
Trial 1	1.36	3.00	58.1	123
Trial 2	3.83	8.45	54.7	116
Trial 3	3.83	8.45	54.7	116
Trial 4	1.36	3.00	43.4	92
Trial 5	2.49	5.50	42.9	91
Trial 6	2.49	5.50	42.9	91
Trial 7	3.83	8.45	64.2	136
Trial 8	3.83	8.45	56.6	120
Trial 9	2.27	5.00	46.7	99

Table 5
ER 5 model trials that vary in load size and air flow rate.

	Load Size		Drum air flow	
	[kg]	[lb]	[L-s^{-1}]	[CFM]
Trial 1	1.36	3.00	51.0	108
Trial 2	5.90	13.0	50.0	106
Trial 3	1.36	3.00	33.0	70
Trial 4	2.49	5.50	32.1	68
Trial 5	5.90	13.0	29.7	63
Trial 6	1.36	3.00	67.5	143
Trial 7	2.49	5.50	67.0	142
Trial 8	5.90	13.0	62.3	132

(BDW) of the load. Fig. 7 shows all trials with the dimensionless airflow parameter $\alpha = 0.9$ (defined in Section 4). These trials also have residence times (τ) falling into the narrow range of 3.91–4.33 s. These trials have widely varying load sizes and inlet temperatures. In general, Fig. 7 indicates higher effectiveness with heavier loads and higher inlet temperatures.

In summary, a few general qualitative trends were identified by inspection of the effectiveness data in this section: generally, higher effectiveness is seen with larger loads, longer residence times, and higher drum inlet temperatures. A more quantitative approach that accommodates the multivariate nature of the problem is developed in Sections 4 and 5.

3.3. Measured effects of cloth type

In addition to DOE cloth, two additional load types were investigated. These loads are defined in the 1992 Association of Home Appliance Manufacturers (AHAM) test procedure HLD-1-1992 [26] and the 2009 AHAM test procedure HLD-1-2009 [27]. Table 6 compares these three load types. Both AHAM tests loads are 100% cotton whereas the DOE test load is 50% cotton and 50% polyester. Each load type consists of varying fabric types and items.

Tables 7 and 8 show the tests that were completed with the AHAM 1992 and 2009 test loads. To develop correlations for each load type, 19 trials were used with AHAM 1992 and 22 trials with AHAM 2009 cloth.

Fig. 8 shows the comparison of effectiveness versus RMC for each dryer model for each of the 3 cloth types. For most dryer models the effectiveness is highest for the DOE cloth and lowest for the AHAM 2009 cloth. Loads with the AHAM 1992 cloth usually have an effectiveness between the DOE and AHAM 2009 cloth.

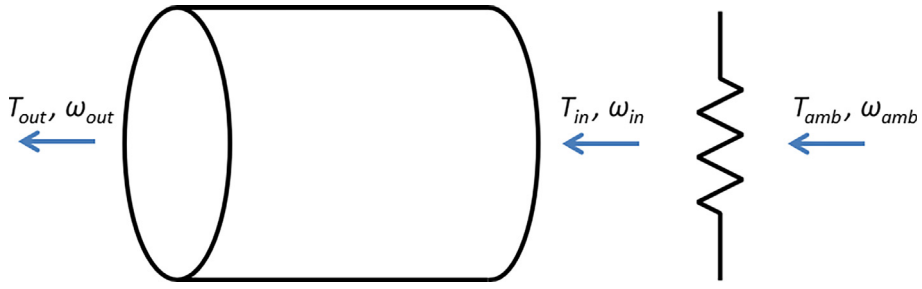

Fig. 4. State points for ambient air entering the dryer cabinet, air entering the drum and air exiting the drum.

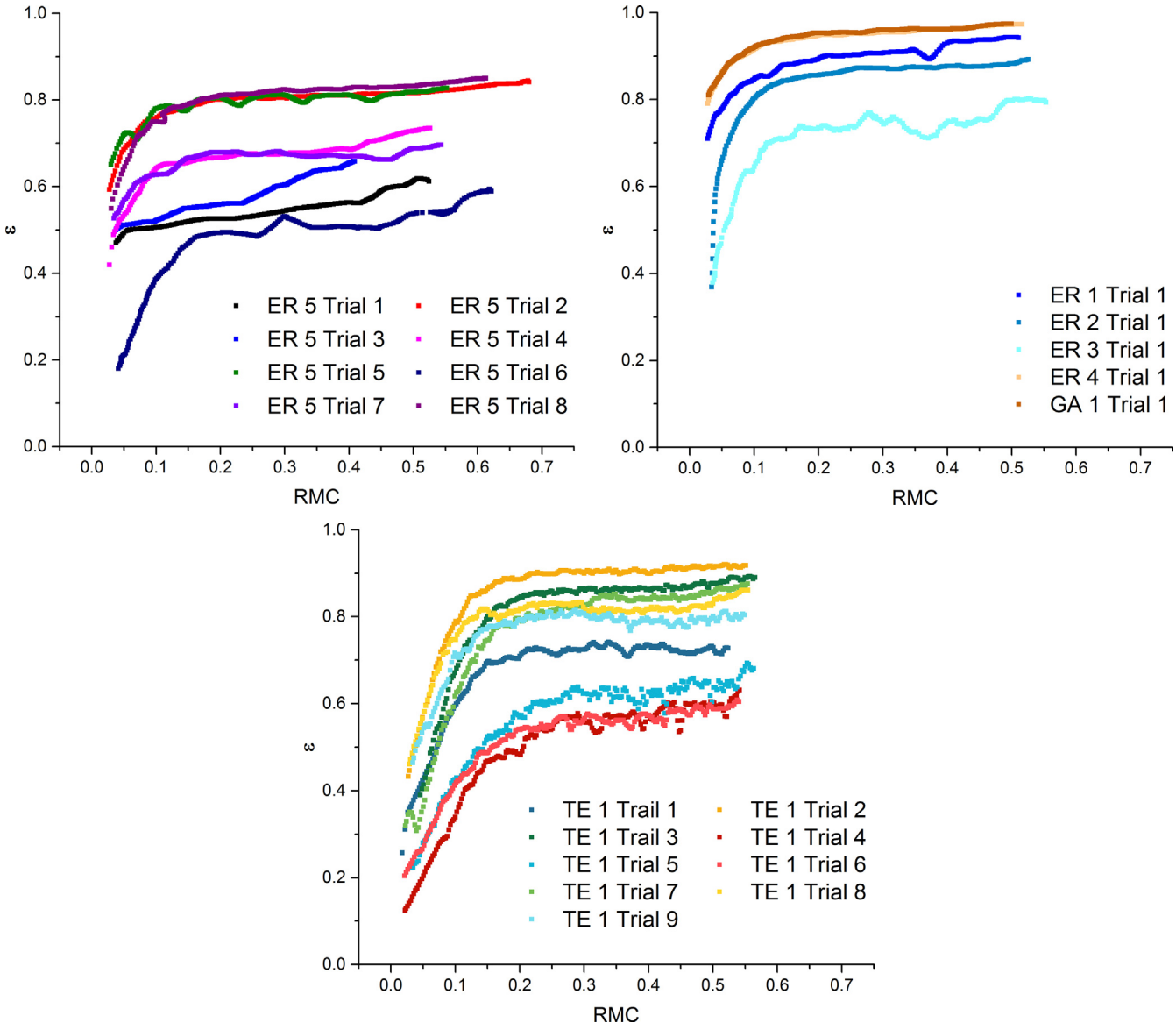

Fig. 5. Effectiveness versus RMC for all trials measured in this work: for dryer ER 5 (a.), dryers ER 1–4 and G 1 (b.), and TE 1 (c.). As the RMC decreases, a transition can be observed from constant rate drying to falling rate drying (around 10–20% RMC).

4. Non-Dimensional analysis

The raw data in Section 3 show a consistent qualitative relationship between effectiveness and RMC. Generally, the effectiveness is fairly constant during the "constant rate drying" phase (from an RMC of 57% down to some transition RMC, typically between 15 and 25%), then declines rapidly during the "falling rate drying" phase with further decrease in RMC. However, the raw data do not readily reveal clear trends in effectiveness with respect to load size, air flow rate, or drum inlet temperature. We pursue a multivariate approach is in this section to capture the influence of these variables.

The objective of this dimensional analysis is to determine a functional relationship between the heat transfer effectiveness in the drum of the clothes dryer and all the variables which affect it. The analysis is applicable for a particular cloth type; the effect of using different cloth types (which have variation in thickness, non-dimensional pressure drop, surface area and wicking ability) is left for future studies. The relationship between heat transfer effectiveness and the corresponding variables can be expressed as shown in Eq. (24),

$$\varepsilon = f\left(t,\ m_{a,d},\ \dot{m}_a, m_c, m_w\right) \tag{24}$$

where ε is the heat and mass transfer effectiveness, t is the fall time (time taken for a piece of cloth to fall from the drum top to the drum bottom), $m_{a,d}$ is the mass of air in the drum at a given instant, $\dot{m}_a$ is the mass flow rate of air passing through the drum, m_c is the mass of the cloth being dried (i.e. load size) and m_w is the mass of the water in the cloth load.

4.1. Determination of Π terms

All variables involved in the problem are first listed. This is accomplished by prior knowledge of clothes drying experiments and physical laws that govern the phenomenon. Next, each variable is expressed in terms of its basic dimensions (M for mass, L for length, and T for time), as shown in Table 9.

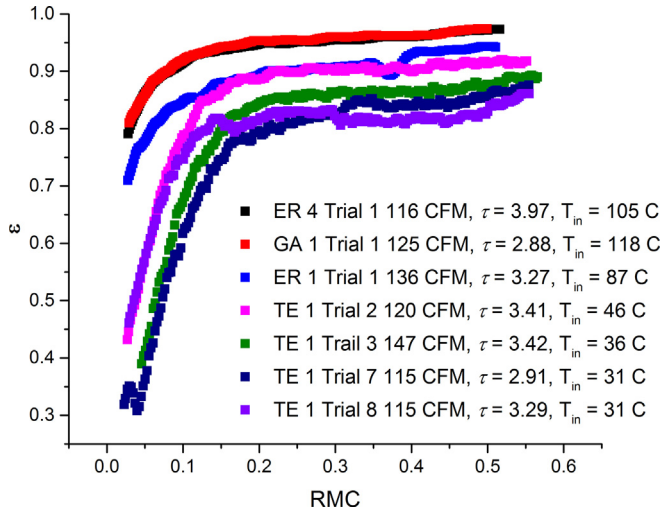

Fig. 6. Effectiveness at different drum residence times and drum inlet temperatures, for all trials with 3.83 kg (8.45 lb) loads.

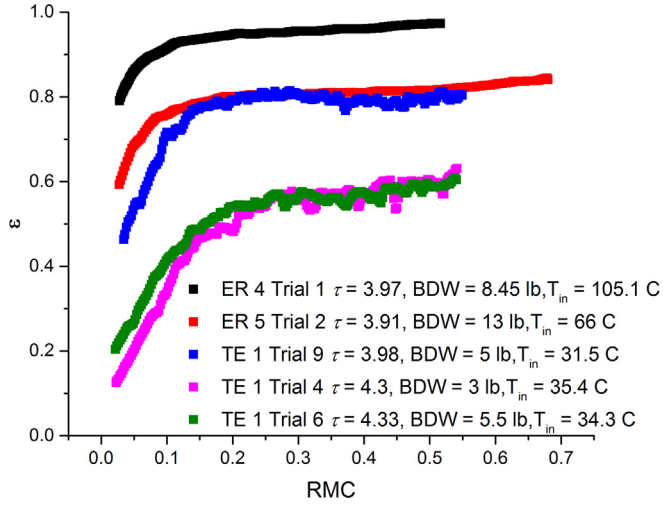

Fig. 7. Effectiveness at different load sizes.

Table 6
Comparison of material in DOE, AHAM 1992 and AHAM 2009 test loads.

	DOE	AHAM 1992	AHAM 2009
Cloth Material	50% Cotton 50% Polyester	100% Cotton	100% Cotton
Fabric Type	Momie Granite	Muslin Broadcloth Terry Combed Cotton	Plain weave linen Huckaback
Individual Items	Towels Wash cloths	Sheets Table cloths Bath towels Long sleeve shirts T-shirts Pillowcases Shorts Wash cloths Handkerchiefs	Sheets Pillowcases Towels

The required number of Π terms is then determined using the Buckingham Pi theorem, as shown in Eq. (25),

$$\#\ of\ \Pi\ terms = k - r \tag{25}$$

where k is number of variables in problem (6) and r is the number of reference dimensions (2). Note that since the heat transfer effectiveness is dimensionless, it is designated Π_1 and its reference dimensions are not used in the Buckingham Pi theorem (they are simply included in Table 9 for completeness). This means the number of reference dimensions for the remaining variables is 2 and, according to Eq. (25), the number of Π terms must be 4. We can rearrange Eq. (24) into the set of nondimensional Π terms as shown in Eq. (26).

$$\Pi_1 = \phi(\Pi_2, \Pi_3, \Pi_4) \tag{26}$$

To determine these Π terms, we use the method of repeating variables. However, as noted above, the effectiveness is itself already nondimensional. Since it does not need to be combined with other variables to form a dimensionless product, we can make it the first Π term in our analysis, as shown in Eq. (27).

$$\Pi_1 = \varepsilon \tag{27}$$

For the remaining terms, two dimensionally independent repeating variables (equal to the number of reference dimensions) are selected from the original list of variables. For this analysis, the fall time, t, and instantaneous mass of air in the drum, $m_{a,d}$, are chosen as the repeating variables. The second Π term is the product of the first non-repeating variable and the repeating variables raised to unknown exponents x and y, as shown in Eq. (28).

$$\Pi_2 = \dot{m}_a t^x m_{a,d}^y \tag{28}$$

To make the above combination dimensionless, each variable is expressed in its basic dimensions and dimensionally equated as shown in Eq. (29).

$$\left(MT^{-1}\right)(T)^x(M)^y \doteq M^0T^0 \tag{29}$$

Solving for x and y results in 2 equations with 2 unknowns. Solving these by substitution gives us the following pi term shown in Eq. (30).

$$\Pi_2 = \frac{\dot{m}_a t}{m_{a,d}} \tag{30}$$

The Π_2 term can be referred to as the "relative air flow rate", denoted α. In other words, it is the mass flow of air through the drum normalized to $m_{a,d}/t$, where $m_{a,d}/t$ is the mass of air in the drum, per unit time required for a cloth to fall from the top to bottom, assuming cylindrical drum geometry with an axis perpendicular to gravity (i.e. a horizontal axis). With the other parameters held constant, α will be *higher* for any of the following:

- *higher* airflow rate through the drum, $\dot{m}_{da}$
- *smaller* drum volume, V
- *larger* drum aspect ratio (diameter:depth)

Following the same procedure, the product of the second non-repeating variable and the repeating variables raised to unknown exponents x and y is given in Eq. (31).

$$\Pi_3 = m_c t^x m_{a,d}^y \tag{31}$$

Following the same methodology as Eq. (29) gives us Eq. (32).

$$(M)(T)^x(M)^y \doteq M^0T^0 \tag{32}$$

Solving for x and y gives us the third Π term shown in Eq. (33).

Table 7
Dryer cycle data for 5 different model dryers with AHAM 1992 Cloth.

		ER 1	ER 2	ER 3	ER 4	GA 1
Drum Volume	[L]	227	113	113	215	170
	[ft^3]	8	4	4	7.6	6
Drum Depth	[m]	0.749	0.603	0.521	0.762	0.572
	[in]	29.5	23.75	20.5	30	22.5
Load Size(s)	[kg]	3.83	1.36	1.36	3.83	3.83
	[lb]	8.45	3	3	8.45	8.45
Cloth Type		AHAM 1992	AHAM 1992	AHAM 1992	AHAM 1992	AHAM 1992
Volumetric air flow rate	[L-s^{-1}]	69.4	35.4	44.8	54.3	59.0
	[CFM]	147	75	95	115	125
Number of Trials		4	10	2	1	2

Table 8
Dryer cycle data for 5 different model dryers with AHAM 2009 Cloth.

		ER 1	ER 2	ER 3	ER 4	GA 1
Drum Volume	[L]	227	113	113	215	170
	[ft^3]	8	4	4	7.6	6
Drum Depth	[m]	0.749	0.603	0.521	0.762	0.572
	[in]	29.5	23.75	20.5	30	22.5
Load Size(s)	[kg]	3.83	1.36	1.36	3.83	3.83
	[lb]	8.45	3	3	8.45	8.45
Cloth Type		AHAM 2009	AHAM 2009	AHAM 2009	AHAM 2009	AHAM 2009
Volumetric air flow rate	[L-s^{-1}]	69.4	35.4	44.8	54.3	59.0
	[CFM]	147	75	95	115	125
Number of Trials		9	8	2	1	2

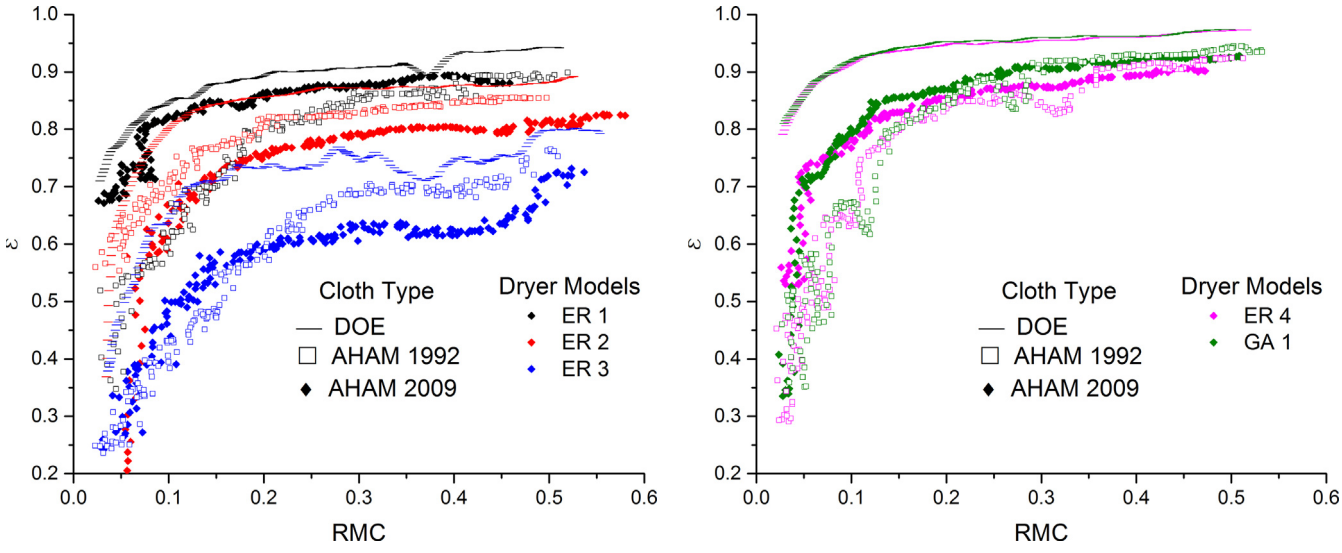

Fig. 8. Selected curves of effectiveness versus RMC for different load types and dryer models. Data symbol type corresponds to load type, and data color corresponds to dryer unit.

Table 9
Expression of each variable in basic dimensions.

Variable	Expression	Expressed in basic dimensions
Heat and mass transfer effectiveness	$\varepsilon = \frac{Q_{actual}}{Q_{max}}$	Dimensionless (ML^2T^{-3}/ML^2T^{-3})
Fall time (related to drum aspect ratio for a horizontal-axis rotating drum)	t	T
Mass of air in drum at standard atmospheric conditions (proportional to drum volume)	$m_{a,d}$	M
Mass flow rate of air	$\dot{m}_a$	MT^{-1}
Mass of cloth (load size)	m_c	M
Mass of water in cloth	m_w	M
Totals	$k = 6$ (number of Variables)	$r = 2$ (M and T are reference dimensions)

$$\Pi_3 = \frac{m_c}{m_{a,d}} \tag{33}$$

The Π_3 term can be referred to as the "relative load size," denoted λ. In other words, λ is the cloth load mass normalized to the mass of air in the drum. With the other parameter held constant, λ will be *higher* for any of the following:

- *larger* load, m_c
- *smaller* drum volume, V

Finally, the product of the third non-repeating variable and the repeating variables raised to unknown exponents x and y is given in Eq. (34).

$$\Pi_4 = m_w t^x m_{a,d}^y \tag{34}$$

The resulting dimensional equation is shown in Eq. (35).

$$(M)(T)^x(M)^y \doteq M^0T^0 \tag{35}$$

Solving for x and y gives us the fourth and final Π term gives Eq. (36).

$$\Pi_4 = \frac{m_w}{m_{a,d}} \tag{36}$$

The Π_4 term can be referred to as the "moisture content," denoted μ. This is directly proportional to the RMC for a given value of λ.

It is important to note the difference between moisture content μ and the commonly used definition RMC. The conventional RMC definition is a mass ratio of cloth moisture to cloth dry weight; whereas moisture content μ is a mass ratio of cloth moisture mass to the mass of air in the drum.

The non-dimensional terms can be summarized as in Table 10.

It is worth noting that this is not the only possible set of terms that can be derived from the same set of premises. Table 11 shows the four possible sets of terms. Our choice, represented in Table 10, appears as the last column in Table 11 (for repeating variables t and $m_{a,d}$). It was chosen for convenience (see last row in Table 11).

The functional relationship of Eq. (24) can now be written as in Eq (37).

$$\varepsilon = \phi\left(\frac{\dot{m}_a t}{m_{a,d}}, \frac{m_c}{m_{a,d}}, \frac{m_w}{m_{a,d}}\right) = \phi(\alpha,\ \lambda,\ \mu) \tag{37}$$

The next step in the analysis is to determine the form of the function ϕ, by correlation to experimental data.

4.2. Computation of non-dimensional terms

Table 12 shows the α and λ terms for each of the trials with DOE cloth. The μ term is not shown here, since it varies throughout each cycle as the water load m_w decreases.

5. Correlation

5.1. Global correlation for DOE cloth

As a global expression of Eq. (37), we chose a polynomial form that is fourth order in μ with no cross terms, and linear in α and λ. This results in 7 fitting parameters, as shown in Eq. (38) and Table 13.

$$\varepsilon = a + b_1\alpha + c_1\lambda + d_1\mu + d_2\mu^2 + d_3\mu^3 + d_4\mu^4 \tag{38}$$

As an illustrative example, Fig. 9 shows the calculated effectiveness versus μ for dryer TE 1, Trial 8, with a 4th order polynomial fit in μ (no cross terms).

To find the coefficients of this form, the Generalized Reduced Gradient algorithm (GRG) that is implemented in Excel's solver function was used [28]. Since each trial was a different length, each trial data set was resampled to approximately 200 points before fitting, to avoid weighting the longer trials more than shorter ones in the correlation process. Also, ε and μ were both smoothed using a moving average window of ±30 s. Table 13 shows the coefficients for the global fit of all 22 DOE cloth trials. The root-mean-squared-error (RMSE) of the global fit was 0.0992. Fig. 10 shows the fit between the global regression and the experimental effectiveness. For each trial the effectiveness at 50, 35, 20, and 6% RMC are plotted. Predictions with error higher than ±20% occur more often when the RMC is 6%, revealing that the global regression prediction is less accurate at these lower RMC values. Fig. 11 shows a comparison of the experimental effectiveness to global fit effectiveness for each dryer model (only Trial 4 is shown for ER5, and only Trial 3 for the TE1 model). The global fit is better for some trials compared to others, all typically within ±20% error except in some cases when RMC is 6% or less. This fit accuracy distribution is expected given the reported prediction error of the global fit. Other dependent variables of the effectiveness such as drum inlet temperature were not accounted for in the global fit and could potentially increase the accuracy.

5.2. Piecewise correlation for DOE cloth

Another method to correlating effectiveness to the Π terms is to use a piecewise approach, where the effectiveness is linear with respect to μ until a transition, after which effectiveness has a higher order correlation to μ. This requires the identification of three points on the $\varepsilon(\mu)$ curve shown in Fig. 12: ε and μ at 50% RMC, ε and μ at a transition point, and ε and μ at the origin. The transition point is defined as the moisture content at which Eq. (39) is true. Eq. (39) expresses the condition where the smoothed slope of the effectiveness with respect to moisture content has doubled relative to the initial smoothed slope at 50%RMC.

Table 10
Summary of derived non-dimensional terms.

	Description	Definition	Equivalents
Π_1	Dryer drum effectiveness	ε	
Π_2	Relative air flow rate	$\alpha = \frac{\dot{m}_a t}{m_{a,d}}$	$\alpha = \frac{t}{\tau}$(fall time/res. time)
Π_3	Relative load size	$\lambda = \frac{m_c}{m_{a,d}}$	
Π_4	Moisture content	$\mu = \frac{m_w}{m_{a,d}}$	$\mu = RMC \times \left(\frac{m_c}{m_{a,d}}\right)$; $\mu = RMC \times \lambda$

Table 11
Full set of possible pi terms.

Pi terms	Repeating variables: t, $\dot{m}_a$	Repeating variables: t, m_c	Repeating variables: t, m_w	Repeating variables: t, $m_{a,d}$
Π_1	ε	ε	ε	ε
Non-repeating variable: $\dot{m}_a$	N/A	Air flow relative to load, $\frac{\dot{m}_a t}{m_c}$	Air flow relative to water, $\frac{\dot{m}_a t}{m_w}$	Air flow relative to drum, $\frac{\dot{m}_a t}{m_{a,d}}$
Non-repeating variable: m_c	Load relative to air flow, $\frac{m_c}{\dot{m}_a t}$	N/A	Load relative to water, $\frac{m_c}{m_w}$	Load relative to drum, $\frac{m_c}{m_{a,d}}$
Non-repeating variable: m_w	Water relative to air flow, $\frac{m_w}{\dot{m}_a t}$	Water relative to load (RMC), $\frac{m_w}{m_c}$	N/A	Water relative to drum, $\frac{m_w}{m_{a,d}}$
Non-repeating variable: $m_{a,d}$	Drum relative to air flow, $\frac{m_{a,d}}{\dot{m}_a t}$	Drum relative to load, $\frac{m_{a,d}}{m_c}$	Drum relative to water, $\frac{m_{a,d}}{m_w}$	N/A
Characteristics	Difficult to articulate	All three vary with load size. One varies with RMC. None are fixed for a dryer unit.	All four vary with time.	One varies with load size One varies with RMC One is fixed for a dryer unit $RMC = \mu \times \left(\frac{m_{a,d}}{m_c}\right) \mu = RMC \times \left(\frac{m_c}{m_{a,d}}\right)$

Table 12
The constant variable and Π terms (α, λ) for each trial with DOE cloth.

Model/Trial #	$\dot{m}_a$		t	$m_{a,d}$		m_c		α	λ	$\tau = m_{a,d}/\dot{m}_a$
	[lb/s]	[kg/s]	[s]	[lb]	[kg]	[lb]	[kg]	–	–	[s]
ER 1 Trial 1	0.18	0.082	0.36	0.60	0.272	8.45	3.83	0.11	14.10	3.27
ER 2 Trial 1	0.09	0.041	0.32	0.30	0.136	3.00	1.36	0.10	10.02	3.20
ER 3 Trial 1	0.12	0.054	0.33	0.30	0.136	3.00	1.36	0.13	10.02	2.53
ER 4 Trial 1	0.14	0.064	0.35	0.57	0.259	8.45	3.83	0.09	14.85	3.97
GA 1 Trial 1	0.14	0.064	0.35	0.45	0.204	8.45	3.83	0.12	18.81	2.88
TE 1 Trial 1	0.15	0.068	0.37	0.49	0.222	3.00	1.36	0.12	6.09	3.20
TE 1 Trial 2	0.14	0.064	0.37	0.49	0.222	8.45	3.83	0.11	17.16	3.41
TE 1 Trial 3	0.14	0.064	0.37	0.49	0.222	8.45	3.83	0.11	17.16	3.42
TE 1 Trial 4	0.11	0.050	0.37	0.49	0.222	3.00	1.36	0.09	6.09	4.30
TE 1 Trial 5	0.11	0.050	0.37	0.49	0.222	5.50	2.49	0.08	11.17	4.34
TE 1 Trial 6	0.11	0.050	0.37	0.49	0.222	5.50	2.49	0.09	11.17	4.33
TE 1 Trial 7	0.17	0.077	0.37	0.49	0.222	8.45	3.83	0.13	17.16	2.91
TE 1 Trial 8	0.15	0.068	0.37	0.49	0.222	8.45	3.83	0.11	17.16	3.29
TE 1 Trial 9	0.12	0.054	0.37	0.49	0.222	5.00	2.27	0.09	10.15	3.98
ER 5 Trial 1	0.13	0.059	0.37	0.52	0.236	3.00	1.36	0.10	5.79	3.84
ER 5 Trial 2	0.13	0.059	0.37	0.52	0.236	13.00	5.90	0.09	25.11	3.91
ER 5 Trial 3	0.09	0.041	0.37	0.52	0.236	3.00	1.36	0.06	5.79	5.93
ER 5 Trial 4	0.08	0.036	0.37	0.52	0.236	5.50	2.49	0.06	10.62	6.10
ER 5 Trial 5	0.08	0.036	0.37	0.52	0.236	13.00	5.90	0.06	25.11	6.58
ER 5 Trial 6	0.18	0.082	0.37	0.52	0.236	3.00	1.36	0.13	5.79	2.90
ER 5 Trial 7	0.18	0.082	0.37	0.52	0.236	5.50	2.49	0.13	10.62	2.92
ER 5 Trial 8	0.16	0.073	0.37	0.52	0.236	13.00	5.90	0.12	25.11	3.14

$$\frac{d\varepsilon}{d\mu} = 2\frac{d\varepsilon}{d\mu}\bigg|_{RMC=50\%} \tag{39}$$

Table 13
Fit parameters for 22 DOE cloth trials.

	Coefficient
a	0.270460
b_1	0.783907
c_1	0.007995
d_1	0.159733
d_2	−0.027454
d_3	0.001945
d_4	−0.000049
RMSE	0.0992

Using data from the 22 trials described in this paper, correlations between the three points on the curve and the two Π terms α and λ were found. Since the origin is known and $\mu_{50} = \lambda/2$ is known, the only three parameters that required a correlation were ε_{50}, ε_{trans}, and μ_{trans}. The experimental values of these three parameters for each trial are shown in Table 15. A linear correlation to α and λ for each of these parameters was found using the GRG algorithm. Eqs. (40-42) describe the form of these correlations and Table 14 shows the coefficients after regression with goodness of fit described as RMSE. Fig. 13 shows the goodness of fit for both ε_{50} and ε_{trans}. Fig. 14 shows the goodness of fit for μ_{trans}. Table 15 also shows the predicted ε_{50}, ε_{trans} and μ_{trans} compared to the actual values for each trial.

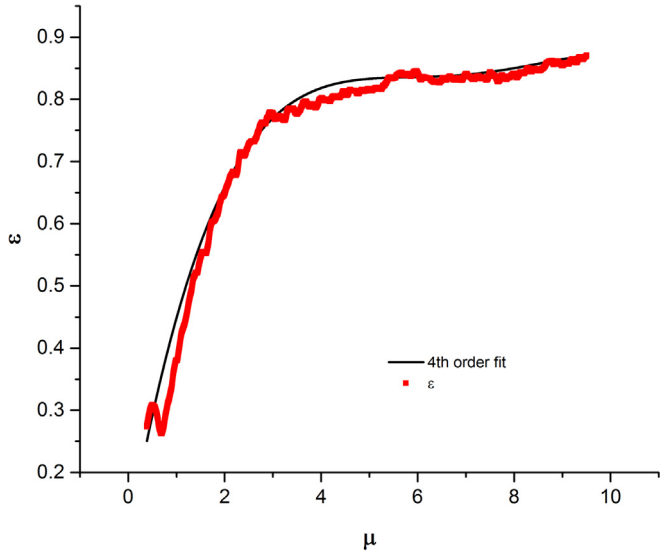

Fig. 9. Example (from one trial) of experimental effectiveness data a curve fit that is 4th order in moisture content μ.

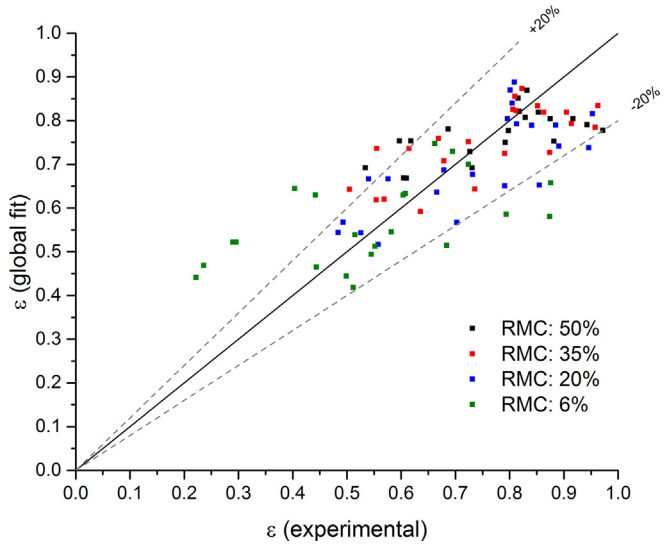

Fig. 10. Global fit vs experimental effectiveness.

$$\varepsilon_{50}(\alpha,\lambda) = a\alpha + c\lambda + d \tag{40}$$

$$\varepsilon_{trans}(\alpha,\lambda) = f\alpha + g\lambda + h \tag{41}$$

$$\mu_{trans}(\alpha,\lambda) = j\alpha + p\lambda + q \tag{42}$$

This framework can be used to predict the effectiveness of a given dryer cycle when α and λ are known and which depend on given dryer drum dimensions, volumetric air flow and load size. The piecewise function in Eq. (43) is used to describe the $\varepsilon(\mu)$ relationship where a linear form describes the effectiveness above ε_{trans} and a fourth order function describes the effectiveness below ε_{trans}.

$$\begin{array}{ll} \varepsilon \geq \varepsilon_{trans} & \varepsilon = m\mu + b \\ \varepsilon < \varepsilon_{trans} & \varepsilon = k(\mu + l)^4 + n \end{array} \tag{43}$$

The following procedure can be used to predict effectiveness based on known α and λ and the coefficients in Table 14.

1. At 50% RMC, find ε_{50} (from Eq. (40) and Table 14) and $\mu_{50} = \lambda/2$.
2. At the transition point, find ε_{trans} (from Eq. (41) and Table 14) and μ_{trans} (from Eq. (42) and Table 14).
3. Eqs. (44-45) can be used to solve for coefficients m and b by assuming $\varepsilon(\mu)$ is linear between $(\mu_{50},\ \varepsilon_{50})$ and $(\mu_{trans}, \varepsilon_{trans})$.

$$m = \frac{(\varepsilon_{50} - \varepsilon_{trans})}{\left(\frac{\lambda}{2} - \mu_{trans}\right)} \tag{44}$$

$$b = \varepsilon_{50} - m\frac{\lambda}{2} \tag{45}$$

4. Eqs. (46–48) can be solved simultaneously to find coefficients k, l and n by assuming $\varepsilon(\mu)$ is fourth order between $(\mu_{trans}, \varepsilon_{trans})$ and $(0, 0)$. A numerical simultaneous equation solution method is recommended due to the high complexity of an analytical solution. Eq. (46) is derived from forcing the 4th order portion of the ε curve to pass through the origin. Eq. (47) is derived from constraining the higher order portion to pass through the point $(\mu_{trans}, \varepsilon_{trans})$. Eq. (48) is derived from constraining the slope of the fourth order form at μ_{trans} to match the slope of the linear portion.

$$0 = k \cdot l^4 + n \tag{46}$$

$$\varepsilon_{trans} = k(\mu_{trans} + l)^4 + n \tag{47}$$

$$m = 4k(\mu_{trans} + l)^3 \tag{48}$$

This procedure was completed to predict the effectiveness for the set of 22 trials. The coefficient k was found to be between −0.2315 and −0.0009, l was found to be between −5.737 and −1.255 and n was found to be between 0.575 and 0.925 for the set of 22 trials. When compared to the experimental effectiveness the RMSE was 0.1186. This is was slightly worse than the global fit presented in Section 5.1, and the piecewise uses 9 fitting parameters where the global fit uses 7. Fig. 15 shows the goodness of fit with ±20% error bars. For each trial the effectiveness at 50, 35, 20, and 6% RMC are plotted, with each RMC noted with a different color. Predictions with error higher than ±20% occur more often when the RMC is 6%. Fig. 16 shows a comparison of the experimental effectiveness to the piecewise fit effectiveness for each dryer model. In comparison with the global fit the linear portion is very similar, however the fourth order shape matches the experimental data better than the global fit. However, the piecewise fit does not fit as well to the linear portion (it is effectively only using 3 fitting parameters to do so). Thus, the piecewise fit has a qualitatively better profile of effectiveness evolution over time, but with a lower overall accuracy. As was discussed for the global fit, the piecewise correlation produced better fit for some trials than others, this is to be expected given the reported accuracy of the correlation.

5.3. Global correlation for AHAM cloths

Global fits for both the AHAM 1992 and 2009 cloth were completed in the same manner as for the DOE cloth presented in Section 5.1 using the polynomial function found in Eq. (38). Table 16 and Table 17 show the coefficients for the global fit and the RMSE for AHAM 1992 and AHAM 2009 cloth. Fig. 17 and Fig. 18 show the

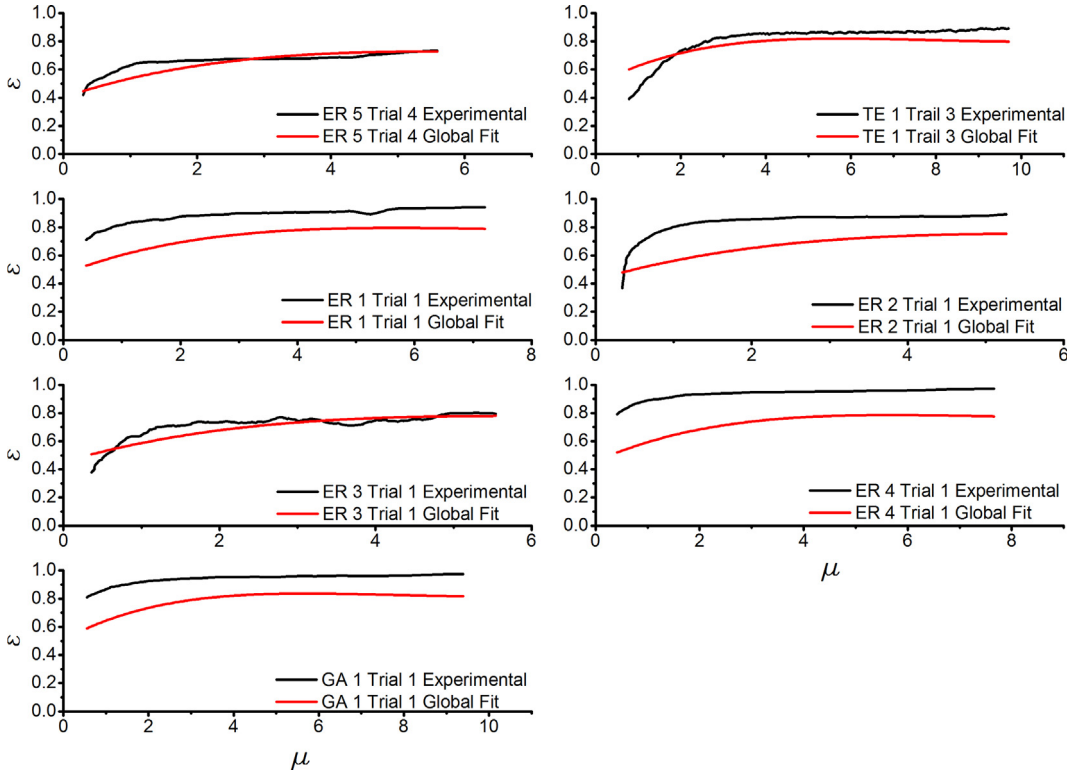

Fig. 11. Comparison of global fit to experimental effectiveness for each dryer model.

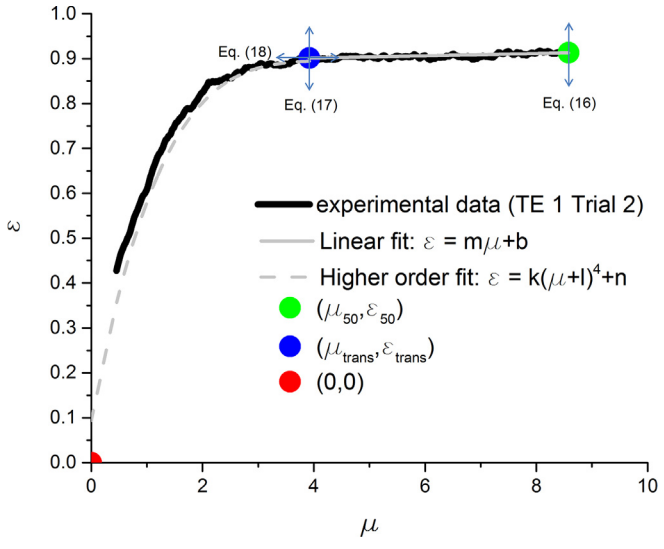

Fig. 12. Piecewise approach illustrated with one example trial. Note that coefficients m, b, k, l, and m are fully specified (have zero degrees of freedom) when the three points (0, 0), (μ_{50}, ε_{50}), and (μ_{trans}, ε_{trans}) are determined.

global effectiveness fit versus the experimental effectiveness for the AHAM 1992 and 2009 load types respectively.

5.4. Discussion of results

Table 18 shows a comparison of the root mean squared error (RMSE) goodness-of-fit for the effectiveness correlations developed in this work.

An interesting observation can be made when comparing the global fit coefficients for each load type, as shown in Table 19. The α term (relative air flow rate) changes sign depending on load type. For the AHAM load types, as α increases the effectiveness decreases, but the reverse is true for the DOE load. This suggests that higher air flow rates only improve effectiveness for the DOE cloth.

6. Conclusions

This work presented a definition of dryer drum heat and mass transfer effectiveness. A dimensional analysis was conducted to establish a functional relationship between the dependent variable effectiveness and the independent variables of load size, drum volume, air flow rate, and drum moisture content. The dimensional analysis defined four non-dimensional terms: drum effectiveness ε, relative air flow rate α, relative load size λ, and moisture content μ.

Empirical data were measured for effectiveness in 7 dryer units,

Table 14
Regressed coefficients from Eqs. (40-42) with goodness of fit described as RMSE.

Dependent variable		Coefficient Value	RMSE in dependent variable (absolute)	RMSE in dependent variable (relative)
ε_{50} (Eq. **(40)**)	**a**	1.496393	0.093	0.122
	c	0.014202		
	d	0.425442		
ε_{trans} (Eq. **(41)**)	**f**	1.296229	0.099	0.134
	g	0.014511		
	h	0.408317		
μ_{trans} (Eq. (42))	**j**	7.828194	0.635	0.243
	p	0.173829		
	q	−0.5752011		

Table 15
Experimental values of ε_{50}, ε_{trans} and μ_{trans} versus values predicted by Eqs. (40-42).

Model and Trial #	Exp. μ_{trans}	Predicted μ_{trans}	Exp. ε_{trans}	Predicted ε_{trans}	Exp. ε_{50}	Predicted ε_{50}	RMC_{trans}
ER 1 Trial 1	2.141	2.729	0.8740	0.7542	0.9294	0.7888	14.64
ER 2 Trial 1	1.326	1.938	0.8085	0.6816	0.8495	0.7153	13.25
ER 3 Trial 1	2.277	2.181	0.7401	0.7217	0.7761	0.7617	22.75
ER 4 Trial 1	2.343	2.696	0.9339	0.7381	0.9626	0.7683	15.87
GA 1 Trial 1	2.629	3.580	0.9313	0.8279	0.9583	0.8618	13.50
TE 1 Trial 1	1.576	1.386	0.7227	0.6462	0.7218	0.6845	25.87
TE 1 Trial 2	4.503	3.253	0.9023	0.7974	0.9152	0.8309	26.25
TE 1 Trial 3	3.725	3.252	0.8507	0.7972	0.8739	0.8306	21.71
TE 1 Trial 4	1.566	1.154	0.5551	0.6077	0.5942	0.6401	25.71
TE 1 Trial 5	2.981	2.030	0.6138	0.6804	0.6363	0.7110	26.69
TE 1 Trial 6	2.742	2.032	0.5529	0.6806	0.5884	0.7114	24.55
TE 1 Trial 7	2.982	3.400	0.7806	0.8218	0.8584	0.8590	17.38
TE 1 Trial 8	2.126	3.284	0.7930	0.8025	0.8328	0.8368	12.39
TE 1 Trial 9	1.540	1.914	0.7735	0.6756	0.7966	0.7082	15.18
ER 5 Trial 1	0.7866	1.180	0.5024	0.6163	0.5872	0.6507	13.83
ER 5 Trial 2	5.236	4.524	0.8007	0.8943	0.8175	0.9224	19.78
ER 5 Trial 3	–	0.9169	–	0.5727	0.5543	0.6004	–
ER 5 Trial 4	1.653	1.743	0.6500	0.6405	0.7020	0.6664	16.18
ER 5 Trial 5	3.552	4.226	0.7868	0.8450	0.8197	0.8655	14.82
ER 5 Trial 6	1.265	1.423	0.4771	0.6564	0.5460	0.6971	19.87
ER 5 Trial 7	2.646	2.255	0.6760	0.7253	0.6779	0.7643	25.09
ER 5 Trial 8	5.291	4.704	0.8093	0.9241	0.8341	0.9568	20.43

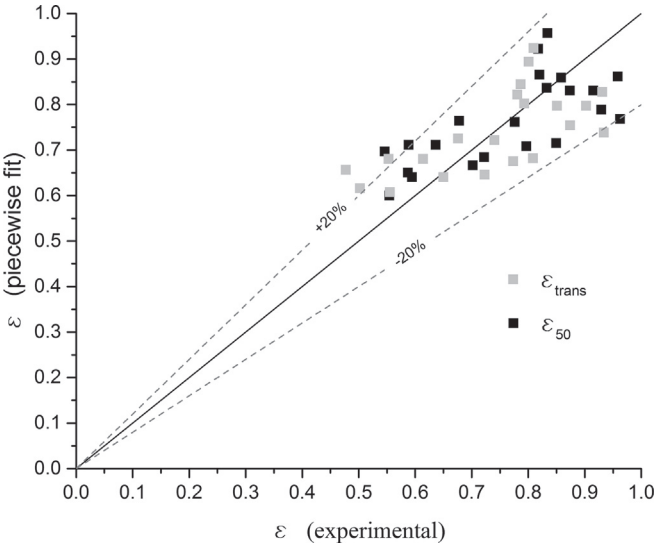

Fig. 13. Goodness of fit for ε_{50} and ε_{trans}.

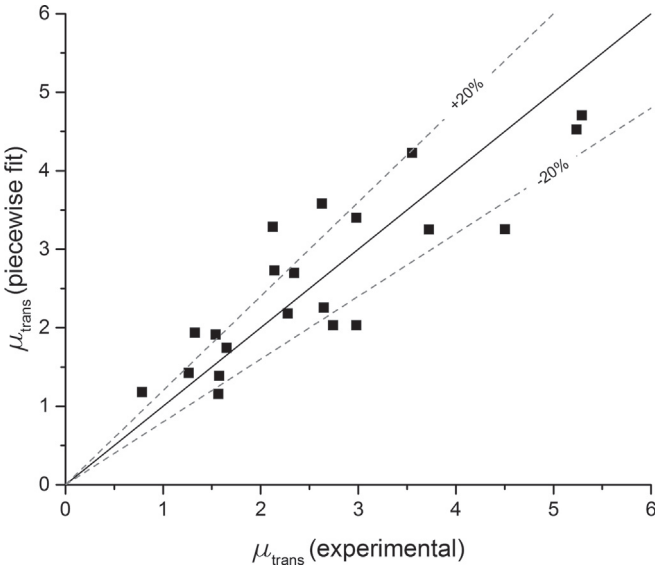

Fig. 14. Goodness of fit for μ_{trans}.

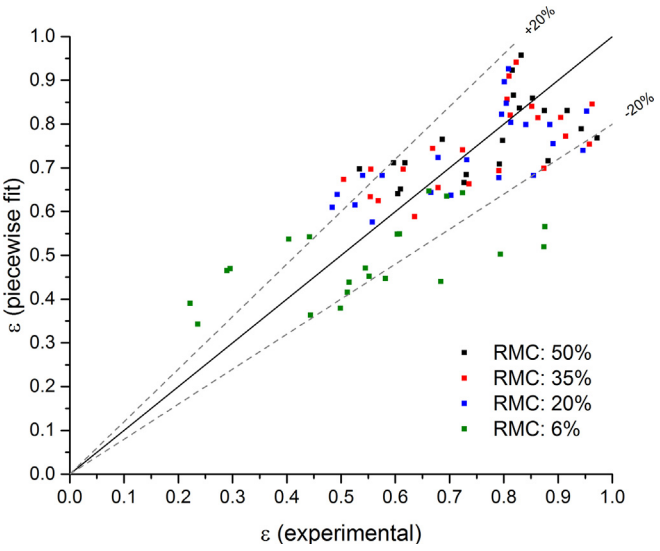

Fig. 15. Piece wise fit vs actual effectiveness.

Table 16
Fit parameters for 19 AHAM 1992 cloth trials.

	Coefficient
a	0.354049
b_1	−2.115320
c_1	0.002120
d_1	0.403633
d_2	−0.087495
d_3	0.008034
d_4	−0.000252
RMSE	0.1040

Table 17
Fit parameters for 22 AHAM 2009 cloth trials.

	Coefficient
a	0.677584
b_1	−4.456546
c_1	0.015385
d_1	0.290916
d_2	−0.071735
d_3	0.007304
d_4	−0.000249
RMSE	0.0572

with 63 instrumented drying trials conducted across three cloth load types (specified in standard test procedures by DOE, AHAM 1992, and AHAM 2009). An uncertainty propagation analysis showed that the experimental procedure to measure effectiveness has a 1.3% uncertainty with respect to instrumentation uncertainties. An analysis of the impact of unmeasured leakage effects showed the empirical procedure to be within 3% accuracy in effectiveness for all practical combinations of unmeasured leakage.

Correlations were presented to establish an empirical relationship between the effectiveness and the derived non-dimensional terms. Two empirical polynomial-based correlation types were pursued: one global, and one piecewise with respect to moisture content. The global fit has slightly better RMSE, however the piecewise fit displayed more consistent trends with qualitatively better shape and may be preferred in some cases. The empirical correlations predicted effectiveness within 0.057–0.119 RMSE for three load types and the two fit types. Errors tended to be larger for low moisture content (low effectiveness).

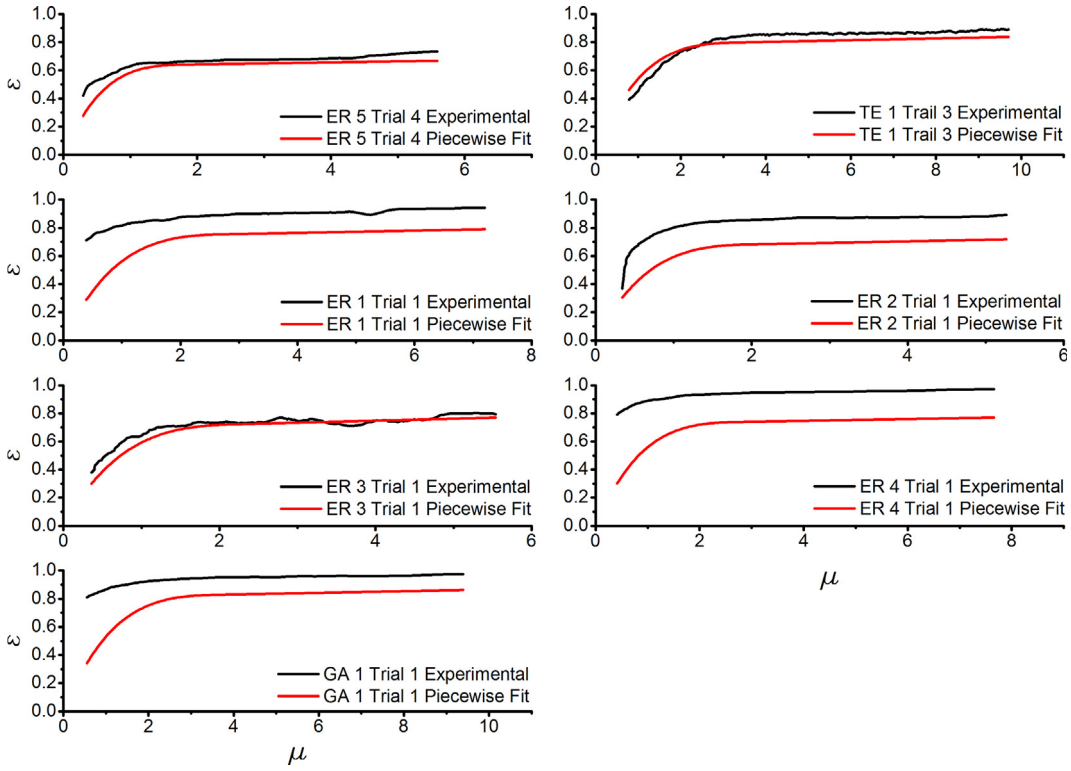

Fig. 16. Comparison of piecewise fit to experimental effectiveness for each dryer model.

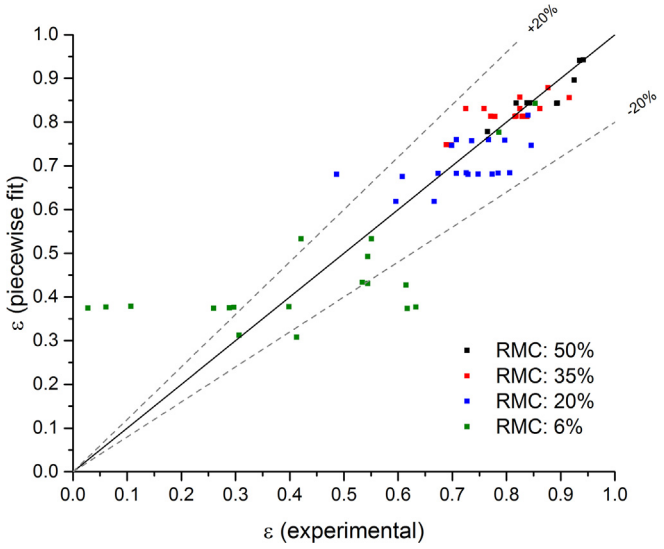

Fig. 17. AHAM 1992 cloth global fit vs experimental effectiveness.

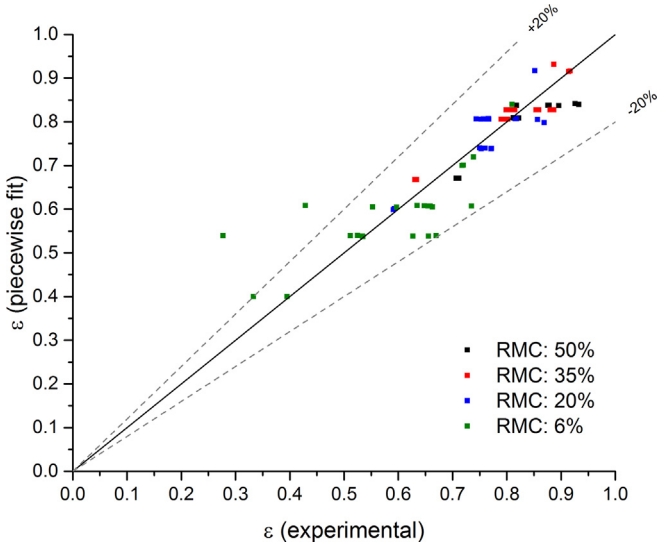

Fig. 18. AHAM 2009 load global fit vs actual effectiveness.

Table 18
Comparison of root mean squared error (RMSE) in effectiveness for the correlations developed in this work.

	DOE	AHAM 1992	AHAM 2009
Global fit	0.099	0.104	0.057
Piecewise fit	0.119	NA	NA

Table 19
Comparison of global fit coefficients for each load type.

Coefficient (Eq. (38))	Variable	2009 AHAM	1992 AHAM	DOE
a	(constant)	0.677584	0.354049	0.27046
$\mathbf{b_1}$	α	−4.456546	−2.11532	0.783907
$\mathbf{c_1}$	λ	0.015385	0.00212	0.007995
$\mathbf{d_1}$	μ	0.290916	0.403633	0.159733
$\mathbf{d_2}$	μ^2	−0.071735	−0.087495	−0.027454
$\mathbf{d_3}$	μ^3	0.007304	0.008034	0.001945
$\mathbf{d_4}$	μ^4	−0.000249	−0.000252	−0.000049

The correlations presented in this work are computationally efficient and can facilitate clothes dryer system modeling (both design models and performance prediction models) by providing a realistic, empirical drum component model for horizontal-axis tumble dryers using standard cloth loads.

Acknowledgements

The authors thank Mr. Antonio Bouza, Technology Development Manager for HVAC, WH, and Appliances, Emerging Technologies Program, Buildings Technology Office at the U.S. Department of Energy for supporting this research. The authors also acknowledge Emily Kirkman for contributions to data processing, Matthew Weathers for discussions of the methodology to compute experimental effectiveness and its uncertainty, Tony Gehl for practical assistance in dryer measurements, Pradeep Bansal for facilitating effectiveness measurements on some models, and test operators Neal Durfee, Geoff Ormston, and Bradley Brown.

Nomenclature

A	area [m^2]
A_t	total area [m^2]
AHAM 1992	cloth load type defined by standard promulgated in 1992 by Association of Home Appliance Manufacturers
AHAM 2009	cloth load type defined by standard promulgated in 2009 by Association of Home Appliance Manufacturers
BDW	bone dry weight of cloth
c_p	specific heat capacity [kJ/kg·K]
DOE	cloth load type defined by standard promulgated by the US Department of Energy
EF	energy factor [lb_{BDW}/kWh]
ER	electric resistance
FMC	final moisture content of cloth (mass ratio of final moisture mass to cloth mass)
G	gas dryer
h	specific enthalpy [kJ/kg]
h_{co}	convective heat transfer coefficient [W/m^2·K]
h_m	mass transfer coefficient [kg/m^2·s]
h_{fg}	heat of vaporization of water [kJ/kg]
J	mass transfer rate [kg/s]
Le	Lewis number [−]
M	mass dimension
NTU	number of transfer units [−]
m_c	dry mass of cloth
m_w	mass of water in cloth
$\dot{m}_{da}$	mass flow rate of dry air circulating through system [kg/s]
$\dot{m}_w$	mass flow rate of water vapor leaving dryer system (net of outflow vs inflow) [kg/s]
P	pressure
Q	heat transfer [kW]
Re	Reynolds number [−]
RH	relative humidity [−]
RMC	remaining moisture content (mass ratio of moisture mass to cloth mass)
SMC	starting moisture content of cloth (mass ratio of initial moisture mass to cloth mass)
T	temperature [°C]; time dimension
V	volume of drum [m^3]
$\dot{V}_{da}$	dry air volume flow rate [m^3/s]
α	relative air flow rate through drum

ε	effectiveness of heat and mass transfer in drum
ε_H	heat transfer effectiveness in drum
ε_M	mass transfer effectiveness in drum
λ	relative load size (mass ratio of cloth mass to drum air mass)
μ	moisture content (mass ratio of moisture mass to drum air mass)
ρ	density [kg/m^3]
τ	residence time of air in drum
ω	humidity ratio [kg_w/kg_{da}]
Π	non-dimensional term derived through systematic dimensional analysis
subscripts	
a	air
atm	atmospheric
0	initial or starting
c	cloth
co	convective
da	dry air
f	final
surf	cloth surface
w	water
out	outlet
in	inlet
max	maximum

References

[1] EIA. Annual energy outlook 2017. U.S. Energy Information Administration; 2017. Online database, https://www.eia.gov/outlooks/aeo/.

[2] Calwell C, Denkenberger D, Spak B, Horowitz N, editors. A call to action for more efficient clothes dryers: U.S. Consumers missing out on $4 billion in annual savings. New York, NY: Natural Resources Defense Council; 2014.

[3] Denkenberger D, Calwell C, Beck N, Trimboli B, Driscoll D, Wold C. Analysis of potential energy savings from heat pump clothes dryers in north America. In: Ecova and collaborative labeling and appliance standards Program (CLASP); 2013.

[4] Lewis WK. The rate of drying of solid materials. Ind Eng Chem 1921;13(5):427–32.

[5] Lewis WK. The evaporation of a liquid into a gas. Trans. ASME. 1922;44:325–40.

[6] Sherwood TK. The drying of solids—I. Ind Eng Chem 1929;21(1):12–6.

[7] Sherwood TK. The drying of solids—II. Ind Eng Chem 1929;21(10):976–80.

[8] Marshall JR,W, Hougen OA. Drying of solids by through circulation. Trans Am Inst Chem Eng 1942;38:91.

[9] Lambert AJD, Spruit FPM, Claus J. Modelling as a tool for evaluating the effects of energy-saving measures. Case study: a tumbler drier. Appl Energy 1991;38(1):33–47.

[10] Deans J. The modelling of a domestic tumbler dryer. Appl Therm Eng 2001;21(9):977–90.

[11] Yi T, Dye JC, Shircliff ME, Ashrafzadeh F. A new physics-based drying model of thin clothes in air-vented clothes dryers. IEEE ASME Trans Mechatron 2016;21(2):872–8.

[12] Bassily AM, Colver GM. Performance analysis of an electric clothes dryer. Dry Technol 2003;21(3):499–524.

[13] Bassily AM, Colver GM. Correlation of the area-mass transfer coefficient inside the drum of a clothes dryer. Dry Technol 2003;21(5):919–44.

[14] Yadav V, Moon CG. Modelling and experimentation for the fabric-drying process in domestic dryers. Appl Energy 2008;85(5):404–19.

[15] Stawreberg L, Nilsson L. Modelling of specific moisture extraction rate and leakage ratio in a condensing tumble dryer. Appl Therm Eng 2010;30(14):2173–9.

[16] Laurijssen J, De Gram FJ, Worrell E, Faaij A. Optimizing the energy efficiency of conventional multi-cylinder dryers in the paper industry. Energy 2010;35(9):3738–50.

[17] Catton W, Carrington G, Sun Z. Exergy analysis of an isothermal heat pump dryer. Energy 2011;36(8):4616–24.

[18] Özahi E, Demir H. A model for the thermodynamic analysis in a batch type fluidized bed dryer. Energy 2013;59:617–24.

[19] Beigi M, Tohidi M, Torki-Harchegani M. Exergetic analysis of deep-bed drying of rough rice in a convective dryer. Energy 2017;140:374–82.

[20] Shen B, Gluesenkamp K, Bansal P, Beers D. Heat pump clothes dryer model development. In: Proc. 16th international refrigeration and air conditioning conference at purdue, west lafayette, IN; 2016.

[21] Patel VK, Gluesenkamp KR, Goodman D, Gehl A. Experimental evaluation and thermodynamic system modeling of thermoelectric heat pump clothes dryer. Appl Energy 2018;217:221–32.

[22] Braun JE, Klein SA, Mitchell JW. Effectiveness models for cooling towers and cooling coils. In: Proc. 1989 ASHRAE annual meeting. Vancouver (Canada): ASHRAE; 1989. p. 164–74.

[23] F-Chart Software. Engineering equation solver. 2016.

[24] Bansal P, Mohabir A, Miller W. A novel method to determine air leakage in heat pump clothes dryers. Energy 2016;96:1–7.

[25] 10 CFR 430, Subpart B. Energy conservation Program for consumer products. In: Test procedures"; appendix D/D1/D2, "uniform test method for measuring the energy consumption of clothes dryers; 2013.

[26] AHAM. Test cloth detailed in AHAM publication HLD-1-1992, household tumble type clothes dryers. Association of Home Appliance Manufacturers; 1992.

[27] AHAM. Test cloth detailed in AHAM publication HLD-1-2009, household tumble type clothes dryers. Association of Home Appliance Manufacturers; 2009.

[28] Lasdon LS, Fox RL, Ratner MW. Nonlinear optimization using the generalized reduced gradient method. Revue française d'automatique, informatique, recherche opérationnelle. Recherche opérationnelle 1974;8(V3):73–103.